



Thermodynamic Analysis of a Power Plant Integrated with Fogging inlet Cooling and a Biomass Gasification

Hassan Athari¹, **Saeed Soltani**^{2*}, **Marc A. Rosen**³, **Seyed Mohammad Seyed Mahmoudi**⁴ and **Tatiana Morosuk**⁵

¹ Department of Mechanical Engineering, University of Ataturk, 25240 Erzurum, Turkey

² Faculty of Mechanical Engineering, University of Tabriz, Iran

³ Faculty of Engineering and Applied Science, University of Ontario Institute of Technology, 2000 Simcoe Street North, Oshawa, Ontario, L1H 7K4, Canada

⁴ Faculty of Mechanical Engineering, University of Tabriz, Iran

⁵ Institute for Energy Engineering, Technische Universität Berlin, Marchstr 18, 10587 Berlin, Germany

E-Mails: hassan.athari@atauni.edu.tr (H.Athari); saeed929@tabrizu.ac.ir (S.Soltani); marc.rosen@uoit.ca (M.A. Rosen); s_mahmoudi@tabrizu.ac.ir (S.M.S Mahmoudi); morozyuk@iet.tu-berlin.de (T. Morosuk)

* Author to whom correspondence should be addressed; Tel.: +98-9144067078; Fax: +98-41-33354153

Received: 7 August 2014 / Accepted: 31 October 2014 / Published: 3 November 2014

Abstract: Biomass energy and especially biofuels produced by biomass gasification are clean and renewable options for power plants. Also on hot days the performance of gas turbines decrease substantially and fog cooling is a useful method for mitigating this problem. In the present paper, a biomass-integrated fogging steam injected gas turbine cycle is analyzed with energy and exergy methods. Increasing the compressor pressure ratio is observed to increase the air flow rate in plant but to reduce the biomass flow rate. Also increasing the gas turbine inlet temperature decreases the air and biomass flow rates. By increasing the pressure ratio the energy and exergy efficiencies increase, especially at lower pressure ratios. Increasing the gas turbine inlet temperature increases the both efficiencies.

Overspray increases the energy efficiency and net cycle power slightly. The gas turbine exhibits the highest exergy efficiency of the cycle components and combustor the lowest. A comparison of the cycle with similar cycles fired by natural gas and differently configured cycles fueled by biomass shows that the cycle with natural gas firing has an energy efficiency 18 percentage points above the biomass fired cycle and that steam injection increases the energy efficiency about 5 percentage points relative to the cycle without steam injection.

Keywords: Biomass; Energy; Exergy; Steam injection; Fog cooler; Gas turbine.

1. Introduction

The performance of a gas turbine, particularly output power and energy efficiency, is significantly affected by ambient temperature. This is especially problematic during hot and humid summer periods when power demands often peak. The cooling of inlet air, which is one of way to increase energy efficiency, involves spraying water droplets into the turbine inlet air to reduce its temperature towards the corresponding wet-bulb temperature. Depending on the injected water amount and injection location, three kinds of fogging systems can be identified:

- High pressure fogging (evaporative fogging) [1]: During the injection of water into the compressor inlet duct, water evaporation is completed before the air enters the compressor.
- Overspray fogging (wet compression) [2-4]: The quantity of water injected into the inlet air exceeds greatly the amount required for air saturation. Hence, a percentage of the water (often ~2%) remains in a liquid phase (i.e., as overspray) and enters the compressor for evaporation there. This method includes a series of high pressure reciprocating pumps providing demineralized water to an array of fogging nozzles located after the air filter elements. The nozzles create a large number of micron size droplets which evaporate, cooling the inlet air to wet bulb conditions.
- Fog intercooling (interstage injection) [5]: The water is injected through the compressor stator blades in order to provide traditional intercooling during compression.

The most advantageous among the available systems is difficult to determine and usually depends on ambient conditions (e.g., ambient air temperature and relative humidity) and design parameters (e.g., air flow rate to gas turbine, power output ratio and number of hours per day in which additional power is needed).

An energy analysis of fogging inlet cooling with overspray demonstrated that inlet air fogging increases the power input to the compressor, reaching the highest value when the inlet air is saturated with moisture [6]. The reason given for this result is that decreasing the inlet air temperature causes an increase in its density and mass flow rate.

Since gas turbines are constant volume machines, at a given shaft speed they move the same volume of air. But the power output of a turbine depends on the flow of mass through it, which is why on hot days, when air is less dense, the power output declines. A 1 °C temperature rise of inlet air leads to a 1% decrease in power output, while increasing the heat rate of the turbine [7].

Steam injection, in which superheated steam is injected into the combustion chamber of a gas turbine, is a useful method for enhancing performance.

It is possible to utilize both techniques through the FSTIG (gas-turbine cycle with steam injection and simultaneous cooling) method. The use of fogging along with steam injection in a gas turbine reduces the inlet air temperature [8]. With this method, the amount of water vapor produced in the boiler is reduced because of the lower temperature of the exhaust gas exiting the turbine. The FSTIG method can modify the performance of cycles by coupling renewable and environmentally benign energy sources. Efforts continue to increase the utilization efficiency of many renewable energy sources [9].

Biomass (e.g., paper, agriculture residue, forestry residue, straw, wood waste, sawdust, paddy husk) can be used as a renewable energy source, and is relatively abundant, clean and carbon dioxide neutral. Biomass can be converted to biofuels via gasification and other methods. Biofuels are usually used for electricity and/or heat generation. Integrated electricity generation cycles that utilize gasification of solid and/or liquid biomass can be environmentally benign and cost effective [10-12]. Nonetheless, biomass fired power plants have some challenges (e.g., relatively low efficiencies), and methods have been proposed in recent years to integrate biomass gasification and natural gas fired gas turbines, to exploit the environmental benefits of the former and the thermal performance and efficiency benefits of the latter [13-17]. But better understanding of such integrated systems is needed before they can be more widely applied, and that is the focus of this work. In the present paper, therefore, the biomass integrated fogging steam injected gas turbine (BIFSTIG) is assessed with energy and exergy analyses. Parametric studies are included to assess the effects of various design parameters on the thermodynamic performance of the cycle. The results are expected to have practical application, since the considered cycle is used for supplying the energy in villages and small towns, especially in tropical locations.

2. Plant description and modeling

2.1. BIFSTIG Plant

In the considered BIFSTIG plant (see Fig. 1), inlet air at ambient conditions (given in Table 1) enters the fogging cooler. The latent heat of vaporization of water is exploited for cooling, since the water is evaporated in the air stream through adiabatic cooling. Hence the cooling energy efficiency is close to 100%. Adiabatic saturation cooling is a process in which air is cooled from the dry bulb temperature to the wet bulb temperature. In this process, the latent heat of vaporization of the water is provided by sensible heat from the air as the water evaporates, reducing in the air stream temperature while

increasing its relative humidity to 100%. Due to overspray (usually up to 2%), water particles often are present at the fog cooler exit. In this study, adiabatic mixing is assumed in the fogging cooler.

Legend:

C	Comp
CC	Combustion chamber
F	Fog cooler
G	Gasifier
GE	Generator
GT	Gas turbine
HSRG	heat recovery steam generator
P	Pump

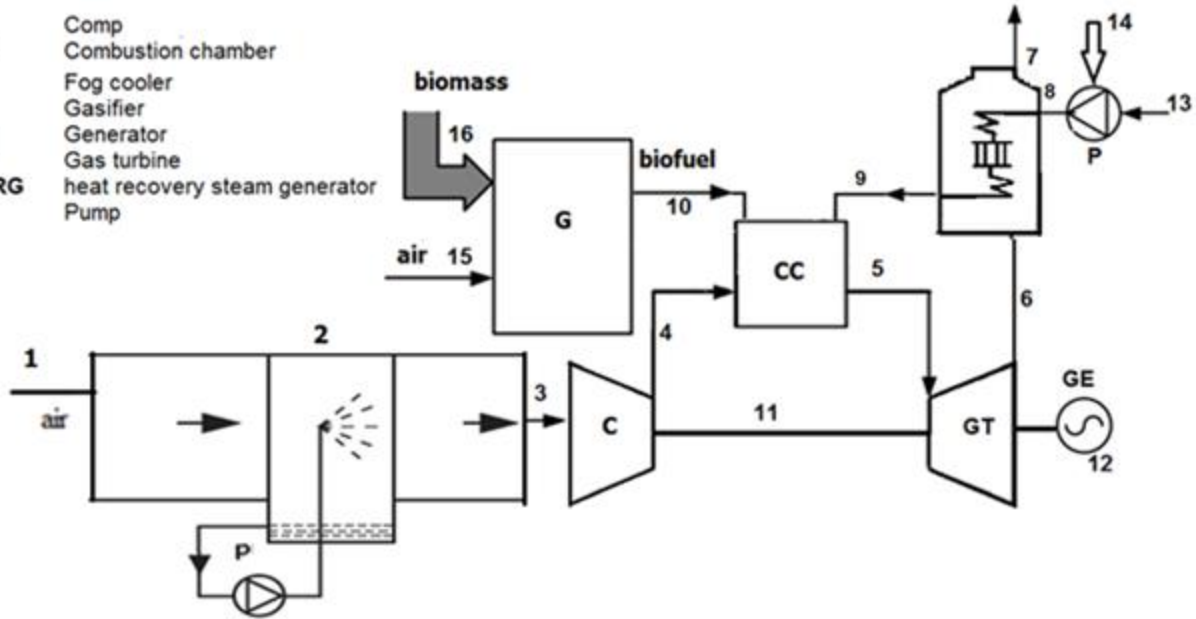


Fig. 1. Gas turbine cycle with steam injection and inlet fogging cooler

The compressor in the BIFSTIG cycle raises the pressure of the saturated air to the combustion chamber pressure. The biomass fuel (wood in the present case) is gasified, and the producer gas from the gasifier enters the combustion chamber. The hot combustion gases expand in the turbine, generating mechanical power, and then enter the heat recovery steam generator (HSRG). There, superheated vapor is produced and for injection into the combustion chamber.

Biomass can be advantageously utilized in this way because biomass-fired gas turbines alone usually cannot attain an adequately high turbine inlet temperature (TIT), while biomass and biofuels have limits regarding system reliability and fuel flexibility.

2.2. Assumptions and data

The assumptions and data which used in the BIFSTIG analyses are listed in Table 1.

Table 1: Assumptions and data used in BIFSTIG analyses

Device or condition	Assumptions and data
Ambient parameters	<ul style="list-style-type: none"> • Inlet air is at atmospheric conditions, i.e., $P_1 = 101.325 \text{ kPa}$, $T_1 = 318 \text{ K}$ and $\phi_{\text{amb}} = 60\%$ • Air composition is 79% nitrogen and 21% oxygen, by vol.

Compressor, turbine, pump	<ul style="list-style-type: none"> • Compressor and turbine polytropic efficiencies are 0.88 [18] • The pump isentropic efficiency is 0.8
Gasifier	<ul style="list-style-type: none"> • The dry biomass (wood) has a gravimetric composition of C: 50%, H: 6% and O: 44%, and a calorific value (on a dry basis) of 449,568 kJ/kmol [19] • The biomass moisture content is 20% on a mass basis • The equivalence ratio for gasification is 0.4188
Heat recovery steam generator	<ul style="list-style-type: none"> • The HRSG steam pressure is 80 bar • The HRSG end temperature difference is 50 K • The pinch point temperature difference in the boiler is 10°C [20]
Combustion chamber	<ul style="list-style-type: none"> • Complete combustion occurs in the combustion chamber • The combustion chamber is adiabatic and has a pressure drop of 1%

The overspray process consists of inlet fogging and wet compression. With inlet fogging, water is injected at approximately 1-2% of the air mass flow rate.

2.3. Thermodynamic modeling and simulation

In modeling and simulating the cycle, mass, energy and exergy balances are written for the BIFSTIG cycle and its components. The exergy analysis considers “Exergy of fuel” and “Exergy of product” [21-25]. Before performing the analysis, it is helpful to define the terms used: \dot{m} , \dot{E} , $\dot{E}_{D,k}$ denote respectively mass flow rate, exergy rate, exergy destruction (irreversibility) rate. The mass and energy balance equations for the all components are summarized by Table 2, but we describe the exergy equations below due to their significance.

Exergy rate balances for the fogging cooler, the compressor and the combustion chamber can be written as follows:

$$\dot{E}_1 + \dot{E}_2 - \dot{E}_3 - \dot{E}_{D,F} = 0 \quad (1)$$

$$\dot{E}_3 + \dot{E}_{11} - \dot{E}_4 - \dot{E}_{D,comp} = 0 \quad (2)$$

$$\dot{E}_4 + \dot{E}_{10} + \dot{E}_9 - \dot{E}_5 - \dot{E}_{D,cc} = 0 \quad (3)$$

where numerical subscripts denote locations identified in Fig. 1.

The turbine inlet temperature (TIT) is determined according to Table 2, using energy analysis and the specified inlet gases for the turbine. To determine the steam injection to the combustion chamber, we define x as the ratio of injected steam from the HRSG to the combustion chamber per 20 kg inlet air mass), and utilize energy equations for the combustion chamber. Thus, the

value of FA (ratio of fuel mass injected from combustion chamber to 20 kg inlet air mass) is obtained. Exergy rate balances for the turbine the heat recovery steam generator and gasifier can be written as:

$$\dot{E}_5 - \dot{E}_6 - \dot{E}_{11} - \dot{E}_{12} - \dot{E}_{D,Turb} = 0 \quad (4)$$

$$\dot{E}_6 + \dot{E}_8 - \dot{E}_7 - \dot{E}_9 - \dot{E}_{D,HRSG} = 0 \quad (5)$$

$$\dot{E}_{16} + \dot{E}_{15} - \dot{E}_{10} - \dot{E}_{D,G} = 0 \quad (6)$$

Table 2: Mass and energy rate balance equations for BIFSTIG cycle components

Component	Mass rate balance	Energy rate balance
Fog cooler	$\dot{m}_f = \dot{m}_a \cdot OS$ $\dot{m}_1 + \dot{m}_2 = \dot{m}_3 + \dot{m}_{f3}$	$ha_3 + w_3 hv_3 + OS \times h_{f3} = ha_1 + w_1 hv_1 + (w_3 - w_1 + OS)h_f$
Compressor	$\dot{m}_3 = \dot{m}_4$	$\int_{T_3}^{T_4} \bar{C}_{P,air} \frac{dT}{T} = \int_{P_3}^{P_4} \frac{\bar{R}}{\eta_{y,comp} P} dP$, $\dot{W}_{comp} = \dot{m}_3 (h_4 - h_3)$
Turbine	$\dot{m}_5 = \dot{m}_6$	$\int_{T_{TOT}}^{T_5} \bar{C}_{P,g} \frac{dT}{T} = \int_{P_6}^{P_5} \eta_{y,turb} \bar{R} \frac{dP}{P}$, $\dot{W}_{turb} = \dot{m}_5 (h_5 - h_6)$
Heat recovery steam generator	$\dot{m}_8 + \dot{m}_6 = \dot{m}_9 + \dot{m}_7$	$\dot{Q}_{HRSG} = \dot{m}_8 \times (h_9 - h_8)$ $(T_7 - T_8) = 50 \text{ K}$ $\dot{Q}_{HRSG} = \dot{m}_s (h_s - h_{w,hrsg})$ $\sum_{Products} n_i \int_{T_7}^{TOT} \bar{C}_{P,g,i} dT = \frac{n_8 [\bar{h}_w(T_9, P_9) - \bar{h}_w(T_8, P_8)]}{\eta_B}$ $x = \frac{n_s \times M_{H_2O}}{\lambda \left(n + \frac{m}{4} \right) \times 4.76 \times (1 + \bar{w}_3) \times M_{air} \times \eta_{cc}}$
Gasifier	$\dot{m}_{15} + \dot{m}_{16} = \dot{m}_{10}$	$\bar{h}_{f_{biomass}}^o + w \times \bar{h}_{f_{H_2O}}^o = n_1 (\bar{h}_{f_{H_2}}^o + \Delta \bar{h}_{H_2}) + n_2 (\bar{h}_{f_{CO}}^o + \Delta \bar{h}_{CO}) + n_3 (\bar{h}_{f_{CO_2}}^o + \Delta \bar{h}_{CO_2}) + n_4 (\bar{h}_{f_{H_2O}}^o + \Delta \bar{h}_{H_2O})$ $+ n_5 (\bar{h}_{f_{CH_4}}^o + \Delta \bar{h}_{CH_4}) + n_6 (\bar{h}_{f_{N_2}}^o + \Delta \bar{h}_{N_2})$

Combustion chamber	$\dot{m}_4 + \dot{m}_9 + \dot{m}_{10} = \dot{m}_5$	$\int_{298.15}^{T_f} \bar{C}_{P,C_nH_m} dT + \lambda(n+m/4) \left[\int_{298.15}^{T_4} \bar{C}_{P,O_2} dT + 3.76 \int_{298.15}^{T_4} \bar{C}_{P,N_2} dT + 4.76\omega_4 \int_{298.15}^{T_4} \bar{C}_{P,H_2O} dT \right] =$ $n \int_{298.15}^{TIT} \bar{C}_{P,CO_2} dT + [\lambda(n+m/4)4.76\omega_4 + m/2] \int_{298.15}^{TIT} \bar{C}_{P,H_2O} dT +$ $3.76\lambda(n+m/4) \int_{298.15}^{TIT} \bar{C}_{P,N_2} dT + (\lambda-1)(n+m/4) \int_{298.15}^{TIT} \bar{C}_{P,O_2} dT - LHV$ $FA = \frac{M_{CH_4}}{\lambda(n+\frac{m}{4}) \times 4.76 \times (1+\bar{w}_2) \times M_{air} \times \eta_{cc}}$
--------------------	--	--

2.4. Validation of results obtained for cycle

The achieved results are validated in two ways. Initially we compare the fogging results with results of others and then the biomass results are compared.

The fogging results obtained in this research are compared with experimental work by Sanaye and Tahani [6]. This comparison is shown in Part A of Table 3, where CIT, CDT, \dot{W}_{net} , TOT and Heat rate denote respectively compressor inlet temperature, compressor discharge temperature, net power production rate of the cycle, turbine outlet gas temperature and cycle heat rate. Next, the results obtained here for biomass gasification are compared with experimental [26] and theoretical [25] work of others. The comparison is shown in Part B of Table 3. For both comparisons, a reasonable agreement is observed.

Table 3: Comparison of reported and computed results for fogging cooler and biomass gasification

Part A: Fogging cooler			Part B: Biomass gasification			
Comparison conditions	Comparison of reported and computed results for selected conditions: TIT = 1122°C, compressor pressure ratio = 11.84, inlet mass rate of turbine = 374.59 kg/s, overspray = 2%		Comparison conditions	Comparison between model and experimental constituent breakdown (in %) for wood at 20% moisture content and a gasification temperature of 800 °C		
Parameter	Reported in [6]	Computed here	Parameter	Computed here	Reported in [26]	Reported in [25]
CIT (°C)	30.00	30.08	Hydrogen	18.01	15.23	21.06

CDT (°C)	293	286.9	Carbon monoxide	18.77	23.04	19.61
\dot{W}_{net} (MW)	133	136	Methane	0.68	1.58	0.64
TOT (°C)	553	577	Carbon dioxide	13.84	16.42	12.01
Heat rate (kJ/kWh)	10,609	10,653	Nitrogen	48.7	42.31	46.68
			Oxygen	0.00	1.42	0.00

3. Results and discussion

The variations with compressor pressure ratio of the biomass and air flow rates are shown in Fig. 2a for the BIFSTIG plant. As pressure ratio increases, the air mass flow rate increases and the biomass flow rate decreases for low values of r_p . At higher values of r_p the curves become flat and even rise. This observation indicates that increasing the compressor pressure ratio increases the size of the power plant. High values of r_p may, consequently, increase the power plant cost due to factors such as the need for thick component wall to withstand the high pressure ratio and the increased cost associated with the air mass flow rate for larger power plants. However, a comprehensive thermoeconomic analysis is needed to determine the actual costs and trends for various cases.

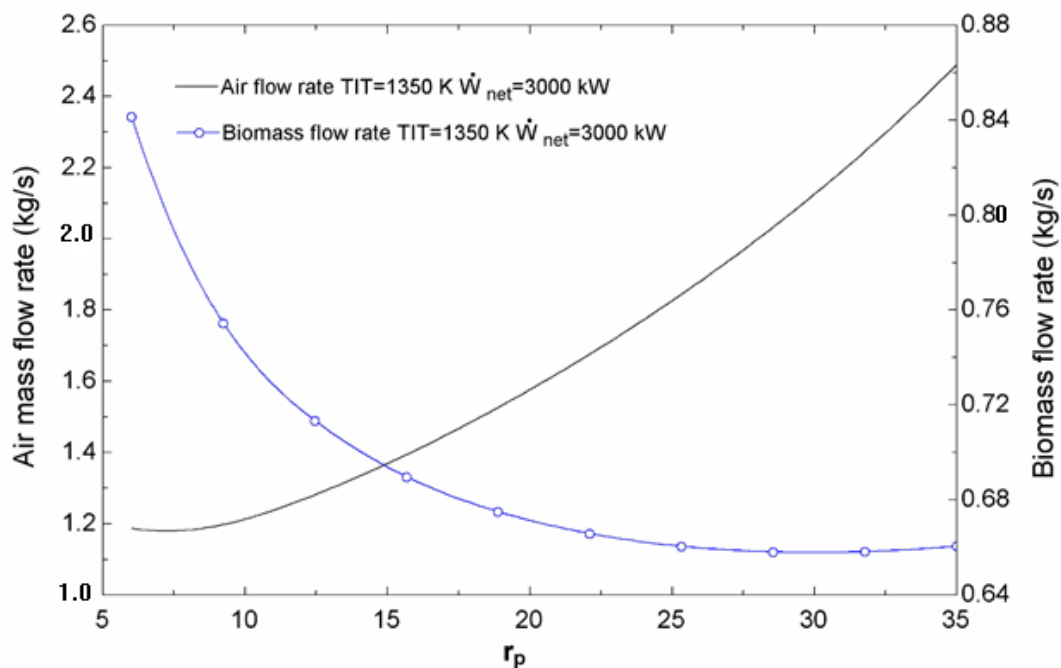


Fig. 2a. Variation of biomass and air mass flow rates with r_p , for the BIFSTIG plant

The variations with gas turbine inlet temperature of biomass and air flow rates are shown in Fig. 2b for the BIFSTIG plant. As TIT increases, the biomass and air mass flow rates decrease, indicating that increasing the TIT decreases the size of power plant. However, as TIT increases the cost of the gas turbine increases. These differing trends make it difficult to ascertain trends with turbine inlet temperature regarding power plant cost, and likely require comprehensive case-dependent thermodynamic and thermoeconomic analyses.

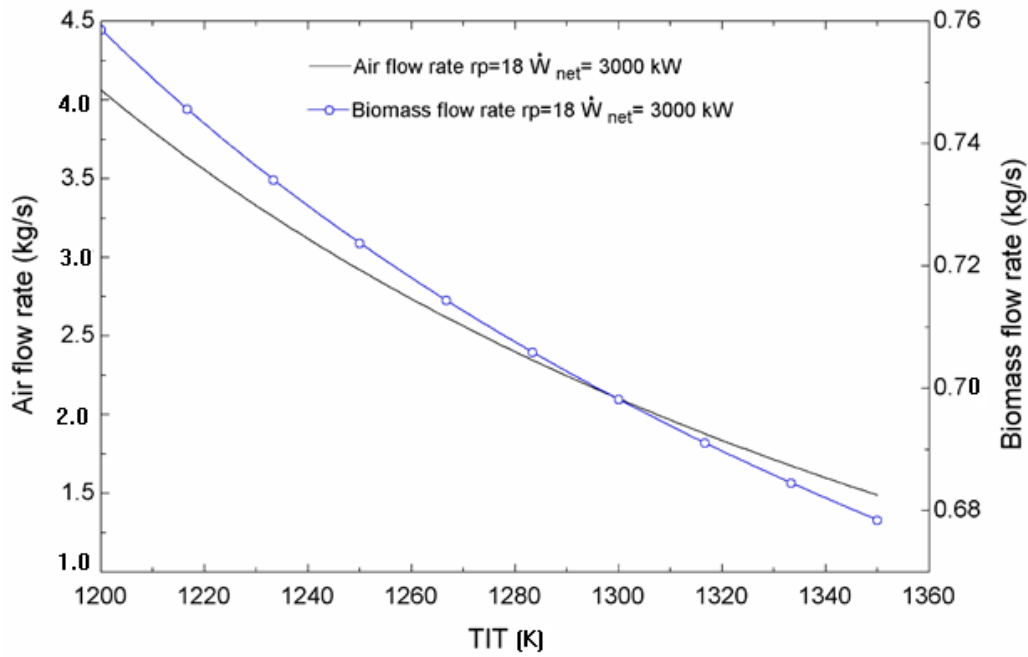


Fig. 2b. Variations of biomass and air mass flow rates with TIT, for the BIFSTIG plant

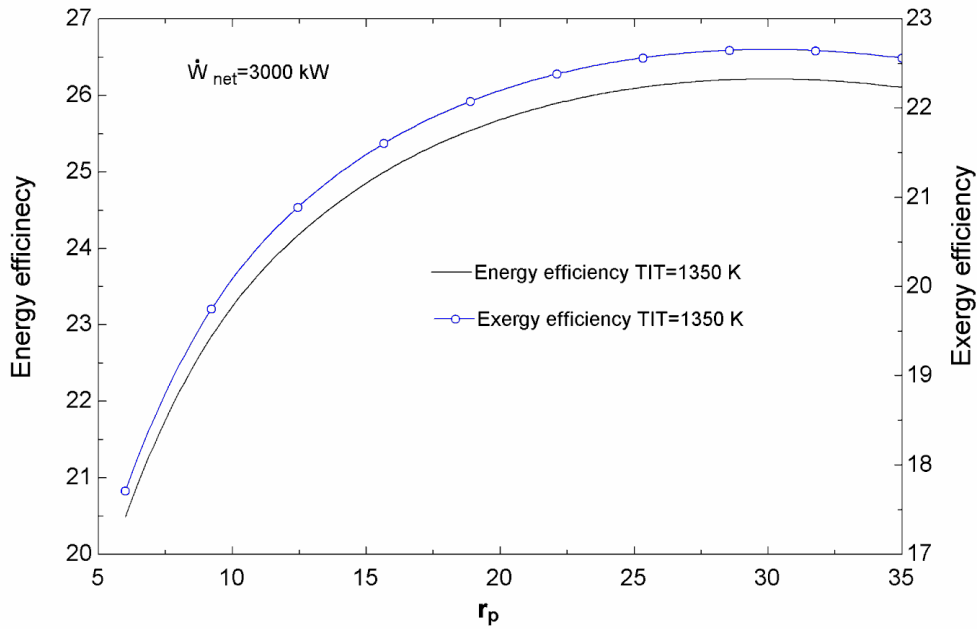


Fig. 3. Variations of energy and exergy efficiencies with r_p , for the BIFSTIG plant

The variations of energy and exergy efficiencies with r_p are shown in Fig. 3 for the BIFSTIG plant. Increasing the compressor pressure ratio raises both efficiencies. The rate of increase with r_p is sharper at lower values of r_p , while at higher values of pressure ratio the increase in energy and exergy efficiencies with r_p is approaches zero and even decreases when $r_p > 30$.

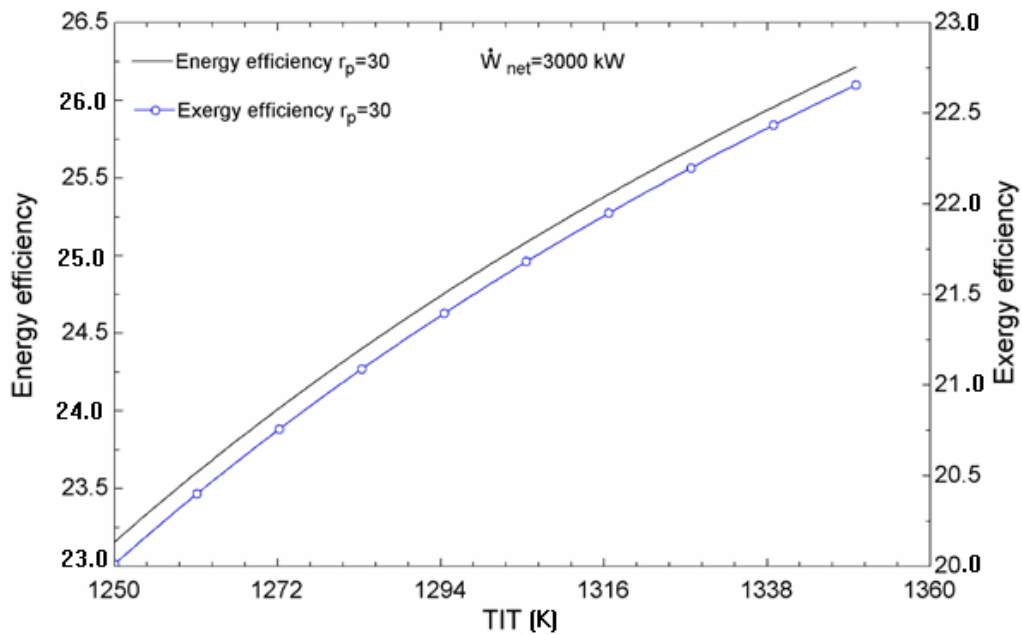


Fig. 4. Variations of energy and exergy efficiencies with TIT, for the BIFSTIG plant

The variations of energy and exergy efficiencies with TIT are shown in Fig. 4 for the BIFSTIG plant. Increasing TIT raises both efficiencies, at roughly the same rate.

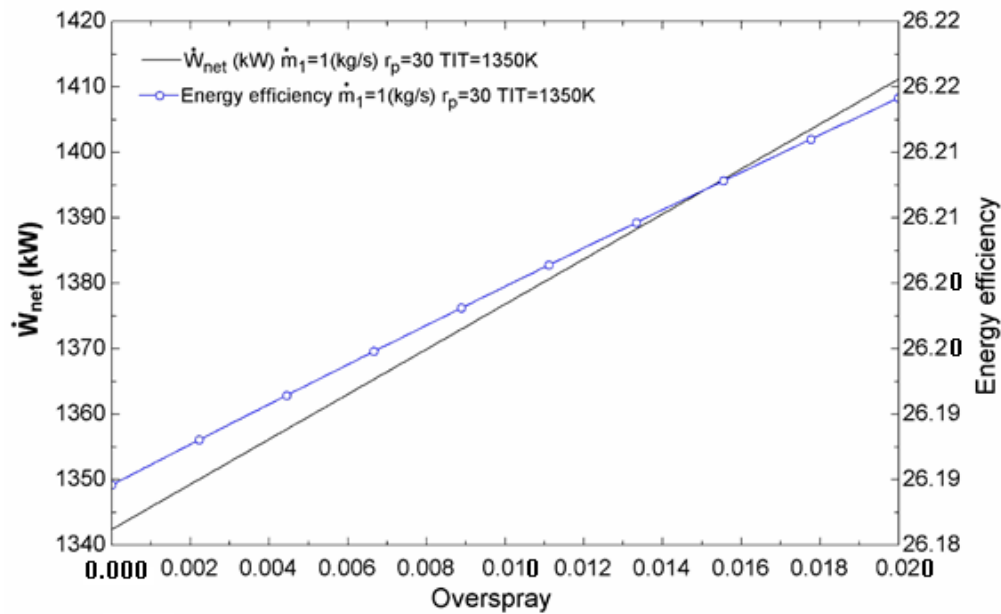


Fig. 5. Variations of net power and energy efficiency with overspray, for the BIFSTIG plant

The variations of net power output and energy efficiency with overspray are shown in Fig. 5 for the BIFSTIG plant. Increasing the overspray raises the net power output and the energy efficiency, but the effect is more pronounced for the net power output. The energy efficiency is only slightly influenced by the level of overspray.

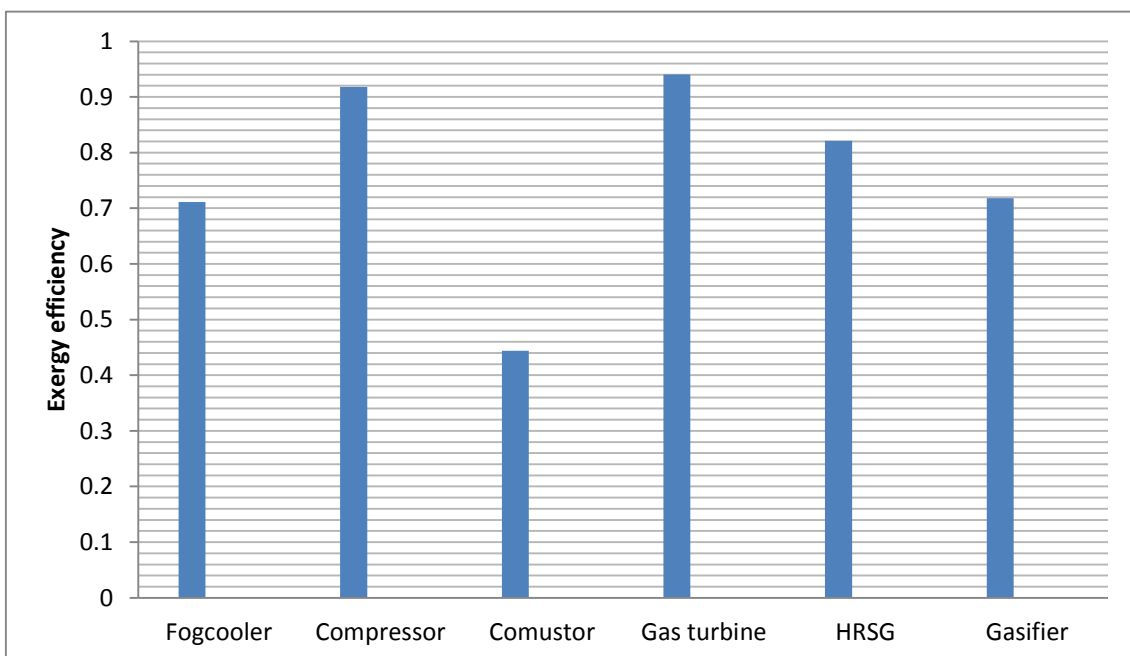


Fig. 6. Exergy efficiencies of components of the BIFSTIG plant, for the maximum energy efficiency condition ($TIT=1350\text{ K}$, $\dot{W}_{net}=3000\text{ kW}$).

Component exergy efficiencies are shown in Fig. 6 for the BIFSTIG plant, for the maximum energy efficiency condition, i.e., for constant value of TIT and net power output. The gas turbine exhibits the highest exergy efficiency and the combustor the lowest. The other components large exergy destruction in the combustor is attributable to the fact that irreversible chemical reactions occur there along with heat transfers across large temperature differences. The large exergy destruction in the fog cooler is attributable to mixing of streams at different temperatures, while the low exergy efficiency of the gasifier is mainly due to chemical reactions in this component.

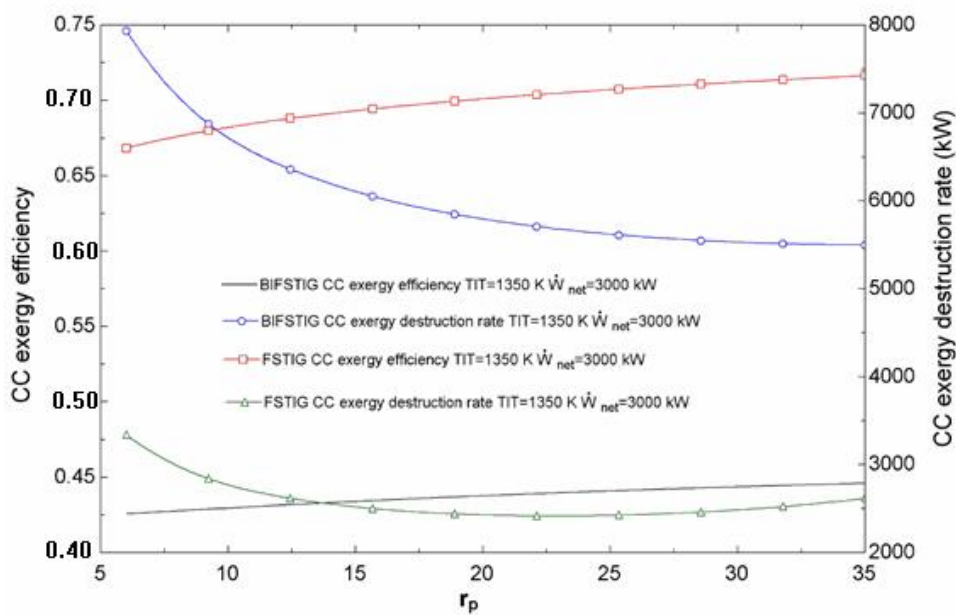


Fig. 7. Variations of combustion chamber (CC) exergy efficiency and exergy destruction rate with r_p , for the BIFSTIG and FSTIG plants

The variations of combustor exergy efficiency and exergy destruction rate with r_p are shown in Fig. 7 for BIFSTIG plant and, for comparative purposes, a FSTIG plant, which is the BIFSTIG configuration except with natural gas as the fuel. This alternative is included to compare the combustion chamber exergy efficiency and exergy destruction rate for these two conditions. Increasing the pressure ratio raises the combustor exergy efficiency and lowers the exergy destruction rate for both cycles. But, the decrease in exergy destruction rate with increasing r_p is sharper for the BIFSTIG than the FSTIG plant. In fact, for the latter case, the exergy destruction rate decreases with pressure ratio to a peak and then increases at higher values of r_p .

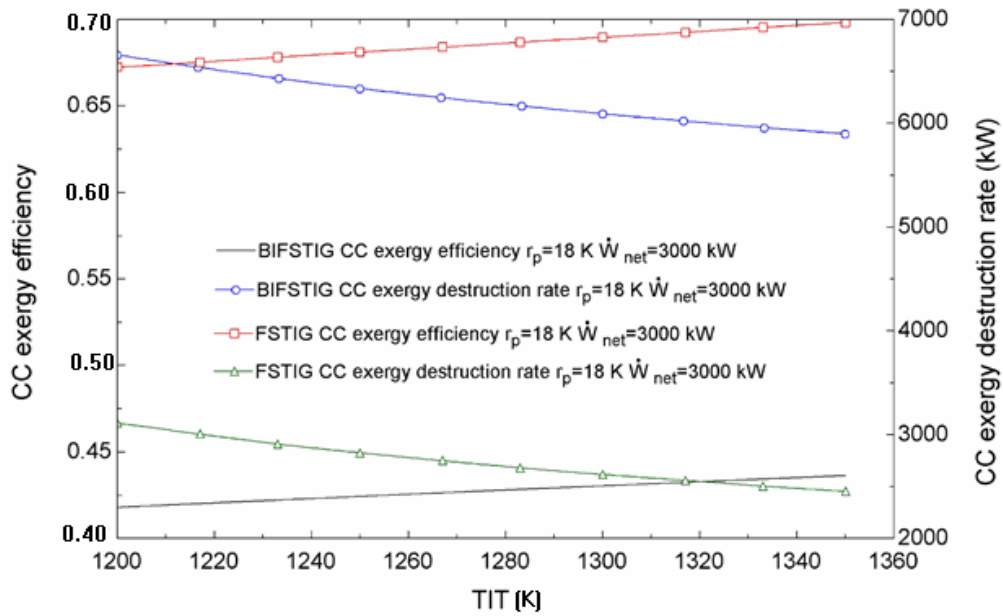


Fig. 8. Variations of combustion chamber (CC) exergy efficiency and exergy destruction rate with TIT, for the BIFSTIG and FSTIG plants

The variations of combustor exergy efficiency and exergy destruction rate with r_p are shown in Fig. 7 for the BIFSTIG and FSTIG plants. An interesting result is shown in Fig. 8, in that increasing TIT raises the combustor exergy efficiency and decreases exergy destruction rate, for both cycles. The combustor exergy efficiency is observed to be higher for the FSTIG plant than the BIFSTIG plant. The lower exergy efficiency for the combustion chamber in the BIFSTIG plant relative to the one in the FSTIG plant constitutes a disadvantage for exploiting biomass in this cycle.

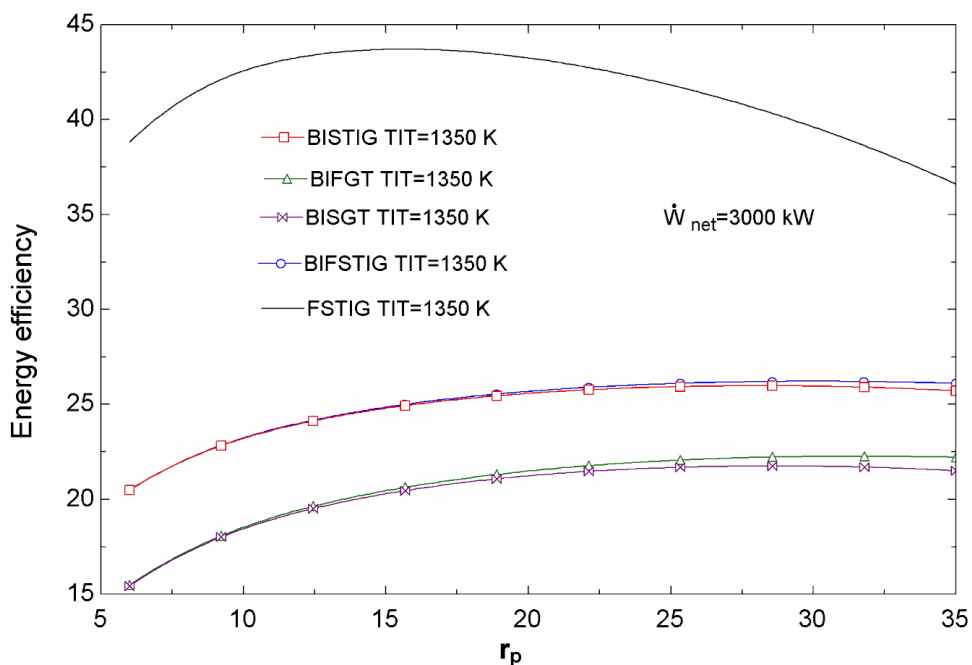


Fig. 9. Variations of energy efficiency with r_p , for various plants

In order to analyze the BIFSTIG plant and its simplified configurations including the FSTIG plant, the variations of energy efficiency with r_p are shown in Fig. 9 for various plants: BIFSTIG (biomass integrated fog cooling steam injection gas turbine), FSTIG (fog cooling steam injection gas turbine with firing of natural gas), BISTIG (biomass integrated gas turbine with steam injection), BIFGT (biomass integrated gas turbine with fog cooling) and BIGT (biomass integrated simple gas turbine). For the FSTIG plant, increasing r_p raises the energy efficiency to a peak, beyond which the energy efficiency decreases. For the BIFSTIG, BISTIG, BIFGT and BISTIG plants, however, increasing the pressure ratio has a notably different influence on the energy efficiency. That is, the efficiency increases sharply with r_p to a value of about 30 and then decreases slightly as r_p increases further.

4. Conclusions

During hot and humid summer periods, when power demand often peaks, compressor inlet cooling is an effective method for offsetting the typical decline in gas turbine performance, while steam injection to the combustion chamber, using steam raised from the turbine exhaust gases in a heat recovery steam generator, is an effective use for the hot gas turbine exit gases. Biomass gasification can be efficiently integrated with a gas turbine cycle for cleaner electricity generation. The biomass integrated fog cooling and steam injection plant gas turbine cycle proposed and analyzed here with energy and exergy methods has significant potential and understanding of its behavior has been improved via the present results. That is, increasing the compressor pressure ratio r_p and gas turbine inlet temperature TIT increases the energy and exergy efficiencies. Also, increasing r_p and TIT decreases the biomass flow rate, while the air mass flow rate increases with increasing r_p and decreases with increasing TIT. Overspray raises the net power output and the energy efficiency, with the influence on former being more significant. Moreover, increasing the r_p and TIT raises the combustor exergy efficiency for the BIFSTIG plant, while increasing the pressure ratio raises the energy efficiency. However, there is an optimum point in terms of a specific pressure value in the natural gas fired plant (FSTIG). For the maximum energy efficiency condition of the BIFSTIG plant, the component exergy efficiency is highest for the turbine and the lowest for the combustor. The BIFSTIG combustor exergy efficiency is lower than for a similar plant fired with natural gas.

Nomenclature

BIFSTIG	Biomass integrated fog cooling steam injection gas turbine
BISTIG	Biomass integrated gas turbine with steam injection
BIFGT	Biomass integrated gas turbine with fog cooling
BIGT	Biomass integrated simple gas turbine
CIT	Compressor inlet temperature ($^{\circ}\text{C}$)

CDT	Compressor discharge temperature ($^{\circ}\text{C}$)
\dot{E}	Exergy rate (kW)
\dot{E}_D	Exergy destruction rate (kW)
FA	Ratio of fuel mass to inlet air mass
FSTIG	Fog cooling steam injection gas turbine with firing of natural gas
h_a	Specific enthalpy of dry air (kJ/kg)
h_v	Specific enthalpies of vapor (kJ/kg)
h_f	Specific enthalpy of water injected into air (kJ/kg)
LHV	Lower heating value (kJ/kg. k)
\dot{m}_a	Mass flow rate of dry air (kg/s)
\dot{m}_f	Mass flow rate of the sprayed water in fogging cooler (kg/s)
\dot{m}_{fuel}	Mass consumption rate of fuel (kg/s)
\dot{m}_i	Mass flow rate of steam at location i (kg/s)
\dot{m}_s	Mass flow rate of steam injected into combustion chamber (kg/s)
\dot{m}_w	Mass flow rate of overspray in fogging cooler (kg/s)
n_s	Molar quantity of steam (mole)
TIT	Turbine inlet temperature (K)
TOT	Turbine outlet temperature (K)
W	Specific humidity (-)
\bar{w}_i	Molar specific humidity per 1 molar of dry air at point i
\dot{W}_{turb}	Outlet power of turbine (kW)
X	Ratio of injected steam from HRSG to 20 kg inlet air mass
Greek Letters	
η_{cc}	Combustion chamber efficiency
λ	Excess air fraction
Subscripts	
Comp	Compressor
CC	Combustion chamber
G	Gasifier
F	Fogging
HRSG	Heat recovery steam generator
i	State point
S	Steam
Turb	Turbine

Conflict of Interest

"The authors declare no conflict of interest".

References and Notes

References

- [1] Bianchi, M.; Melino, F.; Peretto, A.; Bhargava, R. Parametric analysis of combined cycles equipped with inlet fogging. *Journal of Engineering for Gas Turbines and Power* **2006**, 128,326-335.
- [2] Bettocchi, R.; Morini, M.; Pinelli, M.; Spina, P.R.; Venturini, M.; Torsello, G. Setup of an experimental facility for the investigation of wet compression on a multistage compressor. *Journal of Engineering for Gas Turbines and Power* **2011**,133, 102001:(8 pages).
- [3] Ehyaei, M.A.; Mozafari, A.; Alibiglou, M.H. Exergy economic and environmental (3E) analysis of inlet fogging for gas turbine power plant. *Energy* **2011**, 36, 6851-6861.
- [4] Mahto, D.; Pal, S. Thermodynamics and thermo-economic analysis of simple combined cycle with inlet fogging. *Applied Thermal Engineering* **2013**, 51, 413–424.
- [5] Bagnoli, M.; Bianchi, M.; Melino, F.; Peretto, A.; Spina, P.R.; Bhargava, R.; Ingistov, S. A parametric study of interstage injection on GE Frame 7EA gas turbine", *Proceedings of ASME Turbo Expo 2004*, Vienna, Austria, June 14-17, ASME: GT-2004-53042.
- [6] Sanaye, S.; Tahani, M. Analysis of gas turbine operating parameters with inlet fogging and wet compression processes. *Applied Thermal Engineering* **2010**, 30, 234–244.
- [7] Kim, H.; Ko, H.; Perez-Blanco, H. Exergy analysis of gas-turbine systems with high fogging compression. *International Journal of Exergy* **2011**, 8, 16 – 32.
- [8] Kim, H.; Perez-Blanco, H. Potential of regenerative gas-turbine systems with high fogging compression. *Applied Energy* **2007**, 84, 16-28.
- [9] Soltani, S.; Mahmoudi, S.M.S.; Yari, M.; Morosuk, T.; Rosen, M.A.; Zare, V. A comparative exergoeconomic analysis of two biomass and co-firing combined power plants. *Energy Conversion and Management* **2013**, 76, 83–91.
- [10] Park, S.R.; Pandey, A.K.; Tyagi, V.V.; Tyagi, S.K. Energy and exergy analysis of typical renewable energy systems. *Renewable and Sustainable Energy Reviews* **2014**, 30, 105–123.
- [11] Consonni, S.; Larson, ED. Biomass-gasifier/aeroderivative gas turbine combined cycles. Part A-technologies and performance modeling. *J Eng Gas Turbines Power* **1996**, 118, 507–515.

- [12] Faaij, A.; Van Ree, R.; Waldheim, L.; Olsson, E.; Oudhuis, A.; Van Wijk, A.; et al. Gasification of biomass wastes and residues for electricity production. *Biomass and Bioenergy* **1997**, 12(6), 387–407.
- [13] Heidenreich, S.; Foscolo, P.U. New concepts in biomass gasification. *Progress in Energy and Combustion Science* **2014**; DOI: 10.1016.2014.06.002.
- [14] Rodrigues, M.; Andre Faaij, P.C.; Walter, A. Techno-economic analysis of co-fired biomass integrated gasification/combined cycle systems with inclusion of economies of scale. *Energy* **2003**, 28, 1229–1258.
- [15] Tsatsaronis, G.; Pisa, J. Exergoeconomic evaluation and optimization of energy system: application to the CGAM problem. *Energy* **1994**, 9, 287–321.
- [16] Klimantos, P.; Koukouzas, N.; Katsiadakis, A.; Kakaras, E. Air-blown biomass gasification combined cycles (BGCC): System analysis and economic assessment. *Energy* **2009**, 34, 708–714.
- [17] Soltani, S.; Yari, M.; Mahmoudi, S.M.S.; Morosuk, T.; Rosen, M.A. Advanced exergy analysis applied to an externally-fired combined-cycle power plant integrated with a biomass gasification unit. *Energy* **2013**, 59,775-780.
- [18] Rahman Khan, J.; Wang, T. Fog and overspray cooling for gas turbine systems with low calorific value fuels” Proceedings of GT2006ASME Turbo Expo 2006: Power for Land, Sea and Air May 8-11, Barcelona, Spain ASME GT 2006 -90396.
- [19] Robert, H.P.; Don, W.G. *Perry's Chemical Engineers Handbook*, 6th ed.; McGraw Hill: New York, 1984.
- [20] Soltani, S.; Mahmoudi, S.M.S.; Yari, M.; Rosen, M.A. Thermodynamic analyses of an externally fired gas turbine combined cycle integrated with a biomass gasification plant. *Energy Conversion and Management* **2013**, 70, 107–115.
- [21] Moran, M.J.; Shapiro, H.N.; Boettner, D.D.; Bailey, M.B. *Fundamentals of Engineering Thermodynamic*, 7th ed.; Wiley: New York, 2011.
- [22] Dincer, I.; Rosen, M.A. *Exergy: Energy, Environment and Sustainable Development*, 2nd ed.; Elsevier: Oxford, UK, 2013.
- [23] Szargut, J.; Styrylska, T. Approximate evaluation of exergy of fuels. *Brennstoff Warme Kraft* **1964**, 16(12), 589–596.
- [24] Bejan, A. *Advanced Engineering Thermodynamics*, 3rd ed.; Wiley: New York, 2006.
- [25] Zainal, Z.A.; Ali, R.; Lean, C.H. Prediction of performance of downdraft gasifier using equilibrium modeling for different biomass materials. *Energy Convers Manage* **2001**, 42, 1499–1515.

[26] Alauddin, Z.A. *Performance and characteristics of a biomass gasifier system*. PhD thesis, University of Wales, College of Cardiff, UK, 1996.

© 2014 by the authors; licensee MDPI, Basel, Switzerland. This article is an open access article distributed under the terms and conditions of the Creative Commons Attribution license.